Eur. Phys. J. A **19**, 33–44 (2004)
DOI 10.1140/epja/i2003-10111-6

THE EUROPEAN PHYSICAL JOURNAL A

Cranking in isospace

S. Głowacz[1], W. Satuła[1,2,3,4,a], and R.A. Wyss[2,b]

[1] Institute of Theoretical Physics, University of Warsaw, ul. Hoża 69, PL-00 681 Warsaw, Poland
[2] KTH (Royal Institute of Technology), AlbaNova University Center, 106 91 Stockholm, Sweden
[3] Department of Physics, University of Tennessee, Knoxville, TN 37996, USA
[4] Joint Institute for Heavy Ion Research, P.O. Box 2008, MS6374, Oak Ridge, TN 37831, USA

Received: 15 January 2003 / Revised version: 23 May 2003 /
Published online: 18 December 2003 –
Communicated by G. Orlandini

Abstract. The response of isovector and isoscalar pair fields to generalized rotation in isospace is studied. Analytical expressions for constant gap solutions for different limiting cases of the model are derived. In particular, the connections between gauge angles among pairing gaps and the position of the iso-cranking axis are investigated in $N = Z$ nuclei. The two domains of collective and noncollective rotation in space are generalized to isospace. The amplitudes for pair-transfer of $T = 0$ and $T = 1$ pairs are calculated. It is shown that the structure of the $T = 0$ state in odd-odd nuclei prevents any enhancement of pair transfer also in the presence of strong isoscalar pairing correlations. The energy differences of the $T = 0$ and $T = 1$ excitations in odd-odd nuclei are qualitatively reproduced by Total-Routhian-Surface calculations.

PACS. 21.30.Fe Forces in hadronic systems and effective interactions – 21.60.Jz Hartree-Fock and random-phase approximations

1 Introduction

Detailed experimental studies of heavy nuclei along the $N = Z$ line have resulted in a revival of theoretical investigations related to the properties of proton-neutron (pn) pairing correlations [1–13]. In $N = Z$ nuclei one expects short-range correlations of pn type to be of importance due to the fourfold degeneracy of the single-particle (sp) states and the resulting similarity of the spatial components of their wave functions. Of particular interest is the role played by isoscalar ($\boldsymbol{t} = 0$) pairing correlations. It is still an issue of debate to what extent the correlations in this channel of pairing are characterized by a static gap similar to that of the well-established isovector ($\boldsymbol{t} = 1$) pairing interaction.

The aim of our work is to devise a mean-field model in which we can describe consistently excitations in real- and iso-space on the same footing. In a series of papers we have shown that the isobaric analogue states as well as ground-state masses along the $N = Z$ line form a unique probe to $\boldsymbol{t} = 0$ pairing correlations [2,14–17]. Within the mean-field approach, the energy of isobaric analogue states can be described by means of the iso-cranking approximation, analogous to the rotational excitations in real space [15, 18]. The associated broken symmetry is the deformation of the pairing field. The direction of the pairing field vector is determined by the phase angles among the different pair gaps. The calculated excitation spectrum is in turn intimately linked to the direction of the cranking axis in isospace with respect to the pairing field vector. Hereafter (sects. 3 and 4) we derive analytical expressions to elucidate these relations which, in fact, determine the regimes of collective and noncollective rotations in isospace. These expressions and conclusions may be of potential use in other, yet unknown, double-phase paired systems that can be described by means of an external cranking-type Hamiltonian.

The collectivity of pairing correlations can be accessed by means of pair transfer [19]. In the analysis of nuclei in the vicinity of the $N = Z$ line, it was concluded that indeed, the $\boldsymbol{t} = 1$, pn pairing exhibits collectivity [20]. From this analysis, it was suggested that there is little evidence of $\boldsymbol{t} = 0$ collectivity [21]. Let us point out that similar conclusions concerning the role of $\boldsymbol{t} = 0$ pairing have been drawn by the Berkeley group [22] based on the analysis of excitation energy spectra in $N = Z$ nuclei. However, to draw definite conclusions, a detailed understanding of the structure of both $T = 0$ and $T = 1$ ground states in odd-odd (o-o) nuclei as well as the structure of the even-even (e-e) vacuum is necessary. There are empirical arguments based on isobaric symmetry as well as theoretical arguments based essentially on time-reversal symmetry

[a] e-mail: satula@fuw.edu.pl
[b] e-mail: wyss@kth.se

breaking, which indicate that the structures of the lowest $T = 1$ and $T = 0$ states in o-o $N = Z$ nuclei differ [16]. The simplest scenario, within the BCS theory, consistent with the data can be reached by assuming that the wave function of the $T = 0$ state in o-o nuclei is a two–quasi-particle excitation (2QP), whereas the $T = 0$ ground state in e-e nuclei and the lowest $T = 1$ state in o-o nuclei are both local quasi-particle vacua, *i.e.* 0QP states [16]. Within this interpretation the transfer of a $T = 0$ deuteron-like pair will always be strongly quenched, irrespectively of the strength of the $\boldsymbol{t} = 0$ pairing correlations, see sect. 6. Hence, pair transfer may not necessarily be a good indicator for the strength of $\boldsymbol{t} = 0$ pairing correlations.

The outline of the paper is the following: In sect. 3 we derive analytical solutions for the iso-cranked model with $\boldsymbol{t} = 1$ pairing only. In sect. 4 we extend these solutions to include also $\boldsymbol{t} = 0$ pairing. In sect. 5 we discuss the role of the isospin symmetry-breaking mechanism due to number projection and its influence on the Wigner energy. In sect. 6 we discuss pair transfer from $T = 0$ and $T = 1$ states in $N = Z$ o-o nuclei. In sect. 7 we investigate the influence of $\boldsymbol{t} = 0$ pairing on nuclear deformation by performing Total-Routhian-Surface (TRS) type calculations for $T = 0$ and $T = 1$ states in $N = Z$ o-o nuclei. In sect. 8 we discuss briefly the shortcomings of our model due to the lack of the particle-hole isovector field. We summarize and conclude the paper in sect. 9.

2 Invariance of proton-neutron coupled HFB equations

Before going into the details of our model, let us make one general remark concerning proton-neutron coupled HFB equations which will be of relevance for the further discussion. Since, as will be demonstrated later, the solutions of iso-cranking model that include isovector and isoscalar pairing correlations do depend on phase relations between pairing gaps in various channels, it is of importance to notice that the HFB (BCS) equation

$$\begin{pmatrix} \boldsymbol{h} & \boldsymbol{\Delta} \\ -\boldsymbol{\Delta}^* & -\boldsymbol{h}^* \end{pmatrix} \begin{pmatrix} \boldsymbol{U} \\ \boldsymbol{V} \end{pmatrix} = \begin{pmatrix} \boldsymbol{U} \\ \boldsymbol{V} \end{pmatrix} E \tag{1}$$

is invariant under the following transformation:

$$\boldsymbol{U} \longrightarrow \boldsymbol{U} \quad \text{and} \quad \boldsymbol{V} \longrightarrow e^{i\phi}\boldsymbol{V}. \tag{2}$$

Such a transformation changes simultaneously phases of both proton $\boldsymbol{V}_p \rightarrow e^{i\phi}\boldsymbol{V}_p$ and neutron $\boldsymbol{V}_n \rightarrow e^{i\phi}\boldsymbol{V}_n$ amplitudes. Hence, the density matrix and pairing tensor transform as

$$\boldsymbol{\rho} \equiv \boldsymbol{V}^*\boldsymbol{V}^T \longrightarrow \boldsymbol{\rho} \quad \text{and} \quad \boldsymbol{\kappa} \equiv \boldsymbol{V}^*\boldsymbol{U}^T \longrightarrow e^{-i\phi}\boldsymbol{\kappa}, \tag{3}$$

and the single-particle potential $\boldsymbol{\Gamma} \propto \boldsymbol{\rho}$ and pairing potential $\boldsymbol{\Delta} \propto \boldsymbol{\kappa}$ become

$$\boldsymbol{\Gamma} \longrightarrow \boldsymbol{\Gamma} \quad \text{and} \quad \boldsymbol{\Delta} \longrightarrow e^{-i\phi}\boldsymbol{\Delta}. \tag{4}$$

This invariance property allows, for example, to choose one of the pairing gaps to be real. We will take advantage of this transformation property by assuming (apart from sect. 4) that the neutron gap $\Delta_{nn} = \Delta > 0$. However, in some cases and for the sake of simplicity, the eigenvectors will be given only up to the transformation (2).

3 Two-dimensional iso-cranking solutions of the t = 1 pairing model

Let us consider in this section a model Hamiltonian ($\hbar \equiv 1$ for convenience):

$$\hat{H}^{\omega_\tau} = \hat{h}_{\rm sp} - G_{t=1}\hat{\boldsymbol{P}}_1^\dagger\hat{\boldsymbol{P}}_1 - \vec{\boldsymbol{\omega}}_\tau\vec{\hat{\boldsymbol{t}}}, \tag{5}$$

containing isoscalar particle-hole (ph) mean-field $\hat{h}_{\rm sp} = \sum_i e_i(\hat{a}_{in}^\dagger\hat{a}_{in} + \hat{a}_{ip}^\dagger\hat{a}_{ip})$, an isovector $\boldsymbol{t} = 1$ pairing interaction generated by

$$\begin{aligned} \hat{\boldsymbol{P}}_{1\pm1}^\dagger &= \sum_{i>0}\hat{a}_{in(p)}^\dagger\hat{a}_{\bar{i}n(p)}^\dagger \qquad \text{and} \\ \hat{\boldsymbol{P}}_{10}^\dagger &= \frac{1}{\sqrt{2}}\sum_{i>0}(\hat{a}_{in}^\dagger\hat{a}_{\bar{i}p}^\dagger + \hat{a}_{ip}^\dagger\hat{a}_{\bar{i}n}^\dagger), \end{aligned} \tag{6}$$

and two-dimensional iso-rotation $\vec{\boldsymbol{\omega}}_\tau = [\omega_\tau\cos\varphi, \omega_\tau\sin\varphi, 0]$. Planar rotation in $N = Z$ nuclei is the most general since $\langle\hat{t}_z\rangle = 0$ due to number conservation. We are going to consider, for pedagogical reasons, analytical BCS solutions within the constant gap approximation. Moreover, we assume that $\lambda_n = \lambda_p = \lambda$ and $|\Delta_{nn}| = \Delta = |\Delta_{pp}|$, but do not make any further restrictions concerning the phase relations between the gaps. However, the invariance property discussed in the preceding section allows us to choose $\Delta_{nn} = \Delta$ and $\Delta_{pp} = e^{i\alpha}\Delta$ with α being an arbitrary angle. Let us stress here that we will require all phase relations introduced for the pairing gaps at the level of HFB/BCS equations to be rigorously reproduced by our solutions. This requirement will be called *a minimal consistency condition*.

Taking into account the above-mentioned assumptions and constraints, it is straightforward to show that the HFB matrix (1) splits into 8×8 blocks labeled by a single-particle index i. Time-reversal invariance further reduces the problem to the diagonalization of a 4×4 matrix which, in the BCS approximation, *i.e.* after disregarding the contribution from the pairing interaction to the single-particle potential, can be written as

$$\left[\begin{array}{cc|cc} \tilde{e}_i - E_i & -\frac{1}{2}\omega_\tau e^{-i\varphi} & \Delta & e^{i\psi}\Delta_0 \\ -\frac{1}{2}\omega_\tau e^{i\varphi} & \tilde{e}_i - E_i & e^{i\psi}\Delta_0 & e^{i\alpha}\Delta \\ \hline \Delta & e^{-i\psi}\Delta_0 & -\tilde{e}_i - E_i & \frac{1}{2}\omega_\tau e^{i\varphi} \\ e^{-i\psi}\Delta_0 & e^{-i\alpha}\Delta & \frac{1}{2}\omega_\tau e^{-i\varphi} & -\tilde{e}_i - E_i \end{array}\right] \left[\begin{array}{c} U_{\bar{i},n} \\ U_{\bar{i},p} \\ \hline V_{i,n} \\ V_{i,p} \end{array}\right] = 0\,, \tag{7}$$

where $\Delta_{pn} = e^{i\psi}\Delta_0$ ($\Delta_0 = |\Delta_{pn}|$ and ψ denotes an arbitrary angle) and $\tilde{e}_i \equiv e_i - \lambda$. The physical (positive)

eigenvalues of (7) are

$$E_{i\pm} = \sqrt{\tilde{e}_i^2 + \frac{1}{4}\omega_\tau^2 + \Delta_0^2 + \Delta^2 \pm \sqrt{X_i}}\,, \tag{8}$$

where

$$X_i = \tilde{e}_i^2\omega_\tau^2 + 4\Delta^2\Delta_0^2\cos^2\left(\psi - \frac{\alpha}{2}\right) + \omega_\tau^2\Delta^2\sin^2\left(\varphi - \frac{\alpha}{2}\right) - 4\tilde{e}_i\omega_\tau\Delta\Delta_0\cos\left(\varphi - \frac{\alpha}{2}\right)\cos\left(\psi - \frac{\alpha}{2}\right). \tag{9}$$

These roots are double-degenerate (Kramers degeneracy). Having obtained the solution of eq. (7), one can instantly write up the eigenvector for its time-reversed partner. The relation between eigenvectors for time-reversed pairs is best seen when written in the eight-dimensional representation, *i.e.* in the complete representation for a given single-particle index i. It reads:

$$\begin{bmatrix} U_{i\pm,n} \\ U_{i\pm,p} \\ U_{\bar{i}\pm,n} \\ U_{\bar{i}\pm,p} \\ V_{i\pm,n} \\ V_{i\pm,p} \\ V_{\bar{i}\pm,n} \\ V_{\bar{i}\pm,p} \end{bmatrix} : \longrightarrow \begin{bmatrix} 0 \\ 0 \\ U_{\bar{i}\pm,n} \\ U_{\bar{i}\pm,p} \\ V_{i\pm,n} \\ V_{i\pm,p} \\ 0 \\ 0 \end{bmatrix}; \begin{bmatrix} U_{\bar{i}\pm,n} \\ U_{\bar{i}\pm,p} \\ 0 \\ 0 \\ 0 \\ 0 \\ -V_{i\pm,n} \\ -V_{i\pm,p} \end{bmatrix}. \tag{10}$$

3.1 Model including t = 1, $t_z = \pm 1$ pairing

It is pedagogical to consider solutions to the model step by step starting with the standard case without *pn* pairing, $\Delta_0 = 0$. In this case, the eigenvalues (8) become

$$E_{i\pm} = \sqrt{\Delta^2\cos^2\left(\varphi - \frac{\alpha}{2}\right) + \left[\frac{\omega_\tau}{2} \pm \sqrt{\tilde{e}_i^2 + \Delta^2\sin^2\left(\varphi - \frac{\alpha}{2}\right)}\right]^2}. \tag{11}$$

Searching for the eigenvectors we assume that i) satisfactory solutions must obey the *minimal consistency condition*, see above, and reproduce the initial (see eq. (7)) relative phase relation for the gaps: $\Delta_{nn} = e^{-i\alpha}\Delta_{pp}$. ii) Moreover, we assume that neutron and proton amplitudes can differ only by their phase, *i.e.*

$$U_{i,n} = e^{i\zeta}U_{i,p} \quad \text{and} \quad V_{i,n} = e^{i\eta}V_{i,p}\,, \tag{12}$$

which follows from the assumption of charge symmetry for systems described by a common state-independent order parameter Δ. Under these conditions we encounter only two types of solutions:

$$\varphi - \frac{\alpha}{2} = (2k+1)\frac{\pi}{2}, \tag{13}$$

$$\varphi - \frac{\alpha}{2} = (2k)\frac{\pi}{2}. \tag{14}$$

In the first case, $\varphi - \alpha/2 = (2k+1)\pi/2$, the quasiparticle (qp) Routhians (11) become linear as a function of iso-frequency:

$$E_{j\pm} = \left|E_j \pm \frac{1}{2}\omega_\tau\right|, \quad \text{where} \quad E_j = \sqrt{\tilde{e}_j^2 + \Delta^2}. \tag{15}$$

Before the first level crossing, *i.e.* for frequencies lower than

$$\omega_\tau \leq 2E_1 \equiv \omega_\tau^{(1)}\,, \tag{16}$$

where E_1 denotes energy of the lowest qp at frequency zero, the qp Routhians are

$$E_{j\pm} = E_j \pm \frac{1}{2}\omega_\tau. \tag{17}$$

The associated eigenvectors are also independent of ω_τ and equal:

$$\begin{bmatrix} U_{\bar{j}\pm,n} \\ U_{\bar{j}\pm,p} \\ V_{j\pm,n} \\ V_{j\pm,p} \end{bmatrix} : = \begin{bmatrix} U_j \\ \mp e^{i\varphi}U_j \\ V_j \\ \pm e^{-i\varphi}V_j \end{bmatrix}, \tag{18}$$

where the V_j and U_j amplitudes are

$$V_j = \frac{1}{2}\sqrt{1 - \frac{\tilde{e}_j}{E_j}} \quad \text{and} \quad U_j = \frac{1}{2}\frac{\Delta}{\sqrt{E_j(E_j - \tilde{e}_j)}}. \tag{19}$$

For frequencies $\omega_\tau^{(1)} \leq \omega_\tau \leq \omega_\tau^{(2)} \equiv 2E_2$, the standard procedure for blocked states can be applied to calculate eigenvectors, see, *e.g.*, [23] p. 250.

The situation described here is characteristic for a *non-collective* type of rotation. Indeed, in this case the iso-alignment $T = \sqrt{\langle\hat{t}_x\rangle^2 + \langle\hat{t}_y\rangle^2}$ will change stepwise with $\Delta T = 2$ at each crossing frequency $\omega_\tau^{(i)}$, as in the sp model described in detail in refs. [15–17].

The second possibility, (eq. (14)) $\varphi - \alpha/2 = k\pi$, yields Routhians of standard BCS-type:

$$E_{j\pm} = \sqrt{\tilde{e}_{j\pm}^2 + \Delta^2}, \tag{20}$$

where $\tilde{e}_{j\pm} \equiv \tilde{e}_j \pm \frac{1}{2}\omega_\tau$. The eigenvectors are

$$\begin{bmatrix} U_{\bar{j}\pm,n} \\ U_{\bar{j}\pm,p} \\ V_{j\pm,n} \\ V_{j\pm,p} \end{bmatrix} : = \begin{bmatrix} U_{j\pm} \\ \mp e^{i\varphi}U_{j\pm} \\ V_{j\pm} \\ \mp e^{-i\varphi}V_{j\pm} \end{bmatrix}, \tag{21}$$

where

$$V_{j\pm} = \frac{1}{2}\sqrt{1 - \frac{\tilde{e}_{j\pm}}{E_{j\pm}}} \quad \text{and} \quad U_{j\pm} = \frac{1}{2}\frac{\Delta}{\sqrt{E_{j\pm}(E_{j\pm} - \tilde{e}_{j\pm})}}. \tag{22}$$

In this case, the qp Routhians have a nontrivial dependence on ω_τ. They give rise to a smooth alignment typical

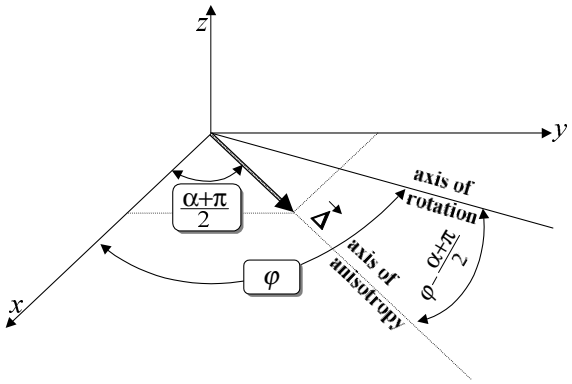

Fig. 1. Schematic drawing showing the relative position of the axis of anisotropy [$\vec{\Delta}$] *versus* axis of iso-rotation. The phase relations (13)-(14) allow either for parallel (noncollective case) or perpendicular (collective case) position of the rotation axes only. Note that tilted solutions are not allowed and hence, three-dimensional iso-cranking in $N = Z$ nuclei can be effectively reduced to one-dimensional theory.

for *collective* rotation. The particular case of this class of solutions corresponding to $\varphi = \alpha = 0$ was discussed in detail in ref. [17].

These two classes of solutions have a simple geometrical interpretation [8,24]. Let us define the vector of anisotropy in isospace $\vec{\Delta} = [\Delta_x, \Delta_y, \Delta_z]$ as

$$\begin{aligned} \Delta_x &= \frac{1}{\sqrt{2}}(\Delta_{pp} - \Delta_{nn})\,; \\ \Delta_y &= \frac{-i}{\sqrt{2}}(\Delta_{pp} + \Delta_{nn})\,; \\ \Delta_z &= \Delta_{pn}\,. \end{aligned} \tag{23}$$

In our case $\Delta_0 = 0$ and

$$\frac{\Delta_x}{\Delta_y} = -\tan\left(\frac{\alpha}{2}\right)\,, \tag{24}$$

as shown schematically in fig. 1. Relations (13)-(14) position the axis of iso-rotation either parallel or perpendicular with respect to $\vec{\Delta}$ giving rise to noncollective or collective iso-rotation, respectively. In particular, for the standard choices of phases $\Delta_{nn} = \pm\Delta_{pp}$, the collective axis is the $x(y)$-axis, respectively. One may summarize that the possible solutions in this case only allow for principal axis cranking. Position of the cranking axis for a desired type of iso-rotation is determined by the relative gauge angle between the neutron and proton pair gap and vice versa.

3.2 Model including complete t = 1 pairing

According to the geometrical interpretation (see fig. 1), switching on *pn* pairing $\Delta_{pn}[\equiv \Delta_z]$ should always induce *collectivity*. Indeed, in this case the qp Routhians (8) would depend on ω_τ in a complicated, nonlinear way for both cases (13) and (14). Closer examination shows in fact, that the *noncollective* solution (18) cannot be generalized to accommodate *pn* pairing, at least not for a general case, see the discussion on a similar subject in sect. 4.2.

This is not surprising, since we deal with planar iso-rotations and the vector representing *pn* pairing is always perpendicular to that plane. The situation resembles that of triaxially quadrupole deformed nuclei, in which cranking around any axis generates a collective spectrum. On the other hand, *collective* solutions (21) can be rather straightforwardly extended to include *pn* pairing. In this case the qp Routhians take the form:

$$E_{j\pm} = \sqrt{\tilde{e}^2_{j\pm} + |\Delta \mp \Delta_0 e^{i(\psi-\varphi)}|^2} \tag{25}$$

and the eigenvectors are

$$\begin{bmatrix} U_{\bar{j}\pm,n} \\ U_{\bar{j}\pm,p} \\ V_{j\pm,n} \\ V_{j\pm,p} \end{bmatrix} : = \begin{bmatrix} U_{j\pm} \\ \mp e^{i\varphi} U_{j\pm} \\ V_{j\pm} \\ \mp e^{-i\varphi} V_{j\pm} \end{bmatrix}\,, \tag{26}$$

where

$$V_{j\pm} = \frac{1}{2}\sqrt{1 - \frac{\tilde{e}_{j\pm}}{E_{j\pm}}} \quad \text{and} \quad U_{j\pm} = \frac{1}{2}\frac{\Delta \mp \Delta_{pn} e^{-i\varphi}}{\sqrt{E_{j\pm}(E_{j\pm} - \tilde{e}_{j\pm})}}. \tag{27}$$

Let us observe that for $\psi - \varphi = (2n+1)\pi/2$ the Routhians (25) have a similar form to the expression derived by Goodman [25] for the static case of $\omega_\tau = 0$:

$$E_{i\pm} = \sqrt{\tilde{e}^2_{i\pm} + \Delta^2 + \Delta_0^2}. \tag{28}$$

For $\psi - \varphi = n\pi$, on the other hand, one gets Routhians similar in structure to those discussed by Bes *et al.* [21]:

$$E_{i\pm} = \sqrt{\tilde{e}^2_{i\pm} + \left(\Delta \mp (-1)^n \Delta_0\right)^2}. \tag{29}$$

To gain further inside into our solutions let us calculate the density matrix:

$$\rho_{i\tau,i\tau} = \rho_{\bar{i}\tau,\bar{i}\tau} = \frac{1}{4}\left\{2 - \frac{\tilde{e}_{i+}}{E_{i+}} - \frac{\tilde{e}_{i-}}{E_{i-}}\right\} \quad \text{for } \tau = n, p\,, \tag{30}$$

$$\rho_{in,ip} = \rho_{\bar{i}n,\bar{i}p} = \frac{e^{-i\varphi}}{4}\left\{\frac{\tilde{e}_{i+}}{E_{i+}} - \frac{\tilde{e}_{i-}}{E_{i-}}\right\}\,, \tag{31}$$

and pairing tensor:

$$\kappa_{jn,\bar{j}n} = e^{-i\alpha}\kappa_{jp,\bar{j}p} = \frac{1}{4}\Delta X_j^{(+)} - \frac{1}{4}\Delta_0 e^{i(\psi-\varphi)} X_j^{(-)}, \tag{32}$$

$$\kappa_{in,\bar{i}p} = \kappa_{ip,\bar{i}n} = \frac{1}{4}\Delta_0 e^{i\psi} X_j^{(+)} - \frac{1}{4}\Delta e^{i\varphi} X_j^{(-)}\,, \tag{33}$$

where

$$X_i^{(\pm)} = \frac{1}{E_{i+}} \pm \frac{1}{E_{i-}} \quad \text{and} \quad X^{(\pm)} = \sum_i X_i^{(\pm)}. \tag{34}$$

Then, the gap equations are

$$\frac{4}{G_{t=1,t_z=\pm1}} = X^{(+)} - \frac{\Delta_0}{\Delta} e^{i(\psi-\varphi)} X^{(-)}\,, \tag{35}$$

$$\frac{4}{G_{t=1,t_z=0}} = X^{(+)} - \frac{\Delta}{\Delta_0} e^{-i(\psi-\varphi)} X^{(-)}\,. \tag{36}$$

For isospin symmetric pairing $G_{t=1,t_z=\pm1} = G_{t=1,t_z=0} = G_{t=1}$ the equations can be solved either when: a) $X^{(-)} = 0$ and for essentially arbitrary values of gaps or b) for $\Delta = \Delta_0$ and $\psi - \varphi = n\pi$. The latter case leads to gapless superconductivity, *i.e.* to an unphysical qp spectrum (29). Indeed, this solution results in a large density of very low-lying 2QP excitations which is not supported by data.

In particular, for the equidistant $e_i = i\delta e$ level model with symmetric cut-off, the particle-hole symmetry leads to $X^{(-)} = 0$, but only for the Routhians of Goodman-type (28). The particle number condition $N = \mathrm{Tr}\rho$ becomes also automatically satisfied since (see eq. (30)):

$$\sum_i \left\{ \frac{\tilde{e}_{i+}}{E_{i+}} + \frac{\tilde{e}_{i-}}{E_{i-}} \right\} \equiv 0. \tag{37}$$

The alignment in isospace is then given by the formula

$$T = \sqrt{\langle \hat{t}_x \rangle^2 + \langle \hat{t}_y \rangle^2} = \frac{1}{2} \sum_{i>0} \left\{ \frac{\tilde{e}_{i+}}{E_{i+}} - \frac{\tilde{e}_{i-}}{E_{i-}} \right\}, \tag{38}$$

which is analogous to the one obtained in ref. [17] (there, Δ^2 should be formally replaced by $\Delta^2 + \Delta_0^2$). Moreover, since for the isospin symmetric model $\Delta^2 + \Delta_0^2$ is constant, the moment of inertia in isospace (MoI-i) and all conclusions drawn there remain unaffected.

For more complex Routhians (*e.g.*, given by eq. (29)) we have not been able to find analytical solutions even for such a high-symmetry model like the equidistant level model.

4 Models including isoscalar pairing

4.1 Pure t = 0 pairing model

Let us now consider the model Hamiltonian

$$\hat{H}^{\omega_\tau} = \hat{h}_{\mathrm{sp}} - G_{t=1} \hat{\boldsymbol{P}}_1^\dagger \hat{\boldsymbol{P}}_1 - G_{t=0} \hat{\boldsymbol{P}}_0^\dagger \hat{\boldsymbol{P}}_0 - \vec{\boldsymbol{\omega}}_\tau \vec{\hat{\boldsymbol{t}}}, \tag{39}$$

consisting of both isovector and isoscalar pairing interactions coupling particles in time-reversed orbits:

$$\boldsymbol{P}_0^\dagger = \frac{1}{\sqrt{2}} \sum_{i>0} (a_{in}^\dagger a_{\bar{i}p}^\dagger - a_{ip}^\dagger a_{\bar{i}n}^\dagger). \tag{40}$$

Let us start our considerations with a pure isoscalar $\boldsymbol{t} = 0$ model. In this case the BCS equations take the following form:

$$\left[\begin{array}{cc|cc} \tilde{e}_i - E_i & -\frac{1}{2}\omega_\tau e^{-i\varphi} & & -\Delta_0 \\ -\frac{1}{2}\omega_\tau e^{i\varphi} & \tilde{e}_i - E_i & \Delta_0 & \\ \hline & \Delta_0^* & -\tilde{e}_i - E_i & \frac{1}{2}\omega_\tau e^{i\varphi} \\ -\Delta_0^* & & \frac{1}{2}\omega_\tau e^{-i\varphi} & -\tilde{e}_i - E_i \end{array}\right] \left[\begin{array}{c} U_{\bar{i},n} \\ U_{\bar{i},p} \\ \hline V_{i,n} \\ V_{i,p} \end{array}\right] = 0\,. \tag{41}$$

Since Δ_0 is the only gap and therefore can be chosen real due to the invariance of HFB equations discussed in sect. 2. The eigenvalues are linear in ω_τ and equal:

$$E_{i\pm} = \left| \frac{1}{2}\omega_\tau \pm E_i \right| = E_i \pm \frac{1}{2}\omega_\tau\,, \qquad \text{where}$$
$$E_i = \sqrt{\tilde{e}_i^2 + \Delta_0^2}\,. \tag{42}$$

The equations are valid below the first crossing frequency $\omega_\tau \leq \omega_\tau^{(1)} \equiv 2E_1$. The roots are double-degenerated due to the Kramers degeneracy. Note, however, that the eigenvectors for pairs of time-reversed states have opposite phase relations between V_i and $V_{\bar{i}}$ amplitudes than for the case of isovector pairing (10). Expressing them in eight-dimensional representation for a given block labeled by the sp index i, we obtain:

$$\begin{bmatrix} U_{i\pm,n} \\ U_{i\pm,p} \\ U_{\bar{i}\pm,n} \\ U_{\bar{i}\pm,p} \\ V_{i\pm,n} \\ V_{i\pm,p} \\ V_{\bar{i}\pm,n} \\ V_{\bar{i}\pm,p} \end{bmatrix} :\longrightarrow \begin{bmatrix} 0 \\ 0 \\ U_i \\ \mp e^{i\varphi} U_i \\ V_i \\ \pm e^{-i\varphi} V_i \\ 0 \\ 0 \end{bmatrix}, \begin{bmatrix} U_i \\ \mp e^{i\varphi} U_i \\ 0 \\ 0 \\ 0 \\ 0 \\ V_i \\ \pm e^{-i\varphi} V_i \end{bmatrix}, \tag{43}$$

where

$$U_i = \frac{1}{2}\sqrt{1 + \frac{\tilde{e}_i}{E_i}} \qquad \text{and} \quad V_i = \frac{1}{2}\sqrt{1 - \frac{\tilde{e}_i}{E_i}} \tag{44}$$

independently of ω_τ. The situation is similar to that described by eqs. (15)-(18) for the case of $\boldsymbol{t} = 1$, $\boldsymbol{t}_z = \pm 1$ pairing in sect. 3.1. However, since the pair field is isotropic in isospace only noncollective iso-rotation takes place regardless of the direction of the iso-cranking axis.

4.2 The t = 0 plus t = 1, $t_z = \pm 1$ pairing model

The extension of the pure $\boldsymbol{t} = 0$ model to include $\boldsymbol{t} = 1$, $\boldsymbol{t}_z = \pm 1$ can be done by linking its solution smoothly to either the *noncollective* solutions (18) or *collective* solutions (21) of the pure $\boldsymbol{t} = 1$ pairing model. Let us consider first *noncollective* solutions obeying the condition (13). These can be relatively easy generalized to include $\boldsymbol{t} = 0$ pairing provided that the following phase relation is satisfied:

$$\theta - \frac{1}{2}\alpha = n\pi\,, \tag{45}$$

where $\Delta_0 = e^{i\theta}|\Delta_0|$. Let us observe that due to the presence of the $\boldsymbol{t} = 1$ field with $\Delta_{nn} = \Delta > 0$ there is only one particular phase relation that allows to choose Δ_0 to be real. This is a necessary condition for the linear term of the determinant of the BCS matrix to vanish and, in turn, to preserve the mirror symmetric structure $[E_i, -E_i]$ of the HFB solutions. In this case, our solutions

have *noncollective* character. The qp Routhians below the first crossing frequency take the following form:

$$E_{i\pm} = E_i \pm \frac{1}{2}\omega_\tau\,, \quad \text{where} \quad E_i = \sqrt{\tilde{e}_i^2 + \Delta^2 + |\Delta_0|^2}. \tag{46}$$

The associated eigenvectors are

$$\begin{bmatrix} U_{i\pm,n} \\ U_{i\pm,p} \\ U_{\bar{i}\pm,n} \\ U_{\bar{i}\pm,p} \\ V_{i\pm,n} \\ V_{i\pm,p} \\ V_{\bar{i}\pm,n} \\ V_{\bar{i}\pm,p} \end{bmatrix} :\longrightarrow \begin{bmatrix} 0 \\ 0 \\ U_{i\pm} \\ \mp e^{i\varphi} U_{i\pm} \\ V_{i\pm} \\ \pm e^{-i\varphi} V_{i\pm} \\ 0 \\ 0 \end{bmatrix}, \begin{bmatrix} -U^*_{i\pm} \\ \pm e^{i\varphi} U^*_{i\pm} \\ 0 \\ 0 \\ 0 \\ 0 \\ V_{i\pm} \\ \pm e^{-i\varphi} V_{i\pm} \end{bmatrix}, \tag{47}$$

where

$$V_{i\pm} = \frac{1}{2}\sqrt{1 - \frac{\tilde{e}_i}{E_i}}\,, \quad \text{and} \quad U_{i\pm} = \frac{1}{2}\frac{\Delta \mp e^{-i\varphi}\Delta_0}{\sqrt{E_i(E_i - \tilde{e}_i)}}\,. \tag{48}$$

However, since the pairing tensors are

$$\kappa_{in,\bar{i}n} = e^{-i\alpha}\kappa_{ip,\bar{i}p} = \frac{\Delta}{2E_i} \quad \text{and} \quad \kappa_{in,\bar{i}p} = -\kappa_{ip,\bar{i}n} = \frac{\Delta_0}{2E_i}\,, \tag{49}$$

the equations for the pairing gaps yield the additional constraint

$$\frac{2}{G_{t=1}} = \sum_{i>0}\frac{1}{E_i} = \frac{2}{G_{t=0}} \tag{50}$$

for the coupling constants. Solutions are therefore possible only for $G_{t=1} = G_{t=0}$. Coexistence of this type was already reported in the literature [1–3].

Generalization of the *collective* solution (13) to include $\boldsymbol{t} = 0$ pairing is far more difficult. It can be shown, however, that for phase relations

$$\theta - \varphi = (2n+1)\frac{\pi}{2}, \tag{51}$$

the eigenvectors take the following form:

$$\begin{bmatrix} U_{i\pm,n} \\ U_{i\pm,p} \\ U_{\bar{i}\pm,n} \\ U_{\bar{i}\pm,p} \\ V_{i\pm,n} \\ V_{i\pm,p} \\ V_{\bar{i}\pm,n} \\ V_{\bar{i}\pm,p} \end{bmatrix} :\longrightarrow \begin{bmatrix} 0 \\ 0 \\ U_{i\pm} \\ \mp e^{i\varphi} U^*_{i\pm} \\ V_{i\pm} \\ \mp e^{-i\varphi} V^*_{i\pm} \\ 0 \\ 0 \end{bmatrix}, \begin{bmatrix} -U^*_{i\pm} \\ \pm e^{i\varphi} U_{i\pm} \\ 0 \\ 0 \\ 0 \\ 0 \\ V^*_{i\pm} \\ \pm e^{-i\varphi} V_{i\pm} \end{bmatrix}. \tag{52}$$

In this case, the qp Routhians are

$$E_{i\pm} = \left(\tilde{e}_i^2 + \frac{\omega_\tau^2}{4} + \Delta^2 + |\Delta_0|^2 \pm 2\sqrt{\frac{\omega_\tau^2}{4}(\tilde{e}_i^2 + |\Delta_0|^2) + \Delta^2|\Delta_0|^2}\right)^{1/2}. \tag{53}$$

For the general case of $\omega_\tau \neq 0$, the amplitudes are given by lengthy and rather nontransparent expressions. However, the property of these solutions are easily recognized already at $\omega_\tau = 0$ when

$$V_{i\pm} = \frac{e^{-i\frac{(\varphi-\theta)}{2}}}{\sqrt{2}}\sqrt{1 - \frac{\tilde{e}_i}{E_{i\pm}}}\cos\frac{\varphi-\theta}{2}\,, \tag{54}$$

$$U_{i\pm} = \frac{e^{-i\frac{(\varphi-\theta)}{2}}}{\sqrt{2}}\frac{\Delta \pm |\Delta_0|}{\sqrt{E_{i\pm}(E_{i\pm} - \tilde{e}_i)}}\cos\frac{\varphi-\theta}{2} \tag{55}$$

and

$$E_{i\pm} = \sqrt{\tilde{e}_i^2 + (\Delta \pm |\Delta_0|)^2}. \tag{56}$$

The gap equations take the following form:

$$\frac{4}{G_{t=1}} = X^{(+)} + \frac{|\Delta_0|}{\Delta}X^{(-)}\,, \tag{57}$$

$$\frac{4}{G_{t=0}} = X^{(+)} + \frac{\Delta}{|\Delta_0|}X^{(-)}\,, \tag{58}$$

where $X^{(\pm)}$ are defined as in eq. (34). Since $X^{(-)} < 0$ the gap equations can be solved only when $G_{t=0} = G_{t=1}$ and $\Delta = |\Delta_0|$. In this case, the qp spectrum takes the unphysical gapless form similar to the case discussed at the end of sect. 3.2.

5 Isospin symmetry breaking

The considerations of sect. 3 show that *collective* isorotations are possible when the isovector pairing field $\vec{\boldsymbol{\Delta}}$ is perpendicular to the axis of iso-cranking. For collective motion the cranking constraint

$$\sqrt{\langle\hat{t}_x\rangle^2 + \langle\hat{t}_y\rangle^2} = T \tag{59}$$

is replaced by

$$\sqrt{\langle\hat{t}_x\rangle^2 + \langle\hat{t}_y\rangle^2} = \sqrt{T(T+1)}. \tag{60}$$

This is a standard procedure that allows to include the effect of isospin fluctuations within the cranked mean-field approximation. Indeed, the microscopic evaluation of this effect would require to go beyond mean-field theory and use, *e.g.*, RPA theory.

Let us observe that the iso-cranking constraint, eq. (60), generates a linear contribution to the symmetry energy, the Wigner energy, $E_{\rm wig} \sim T$. In spite of this linear term, calculations of the measured $T = 2$ states in e-e $N = Z$ nuclei show [15–17] that in the presence of the standard $\boldsymbol{t} = 1$ field, the MoI-i is too large. In other words, the size of the calculated Wigner energy is too small to account for the empirical excitation energy. In these calculations, the mechanism to lower the MoI-i and bring it in agreement with experiment was associated with isoscalar pairing in complete analogy to the mechanism of lowering the spatial MoI by the isovector super-fluidity [15–17].

However, in these calculations the isovector part of the *particle-hole* field was not taken into account [26] (see also sect. 8).

To account for isospin fluctuations by means of the cranking condition (60) and to enlarge (locally, *i.e.* in $N \sim Z$ nuclei) the MoI-i, it is necessary to find a solution that mixes $\boldsymbol{t} = 0$ and $\boldsymbol{t} = 1$ pairing, and is of *collective* type. As demonstrated in sect. 4, at the level of the BCS approximation one cannot obtain such a solution. It has already been shown [2] that the approximate number projection of Lipkin-Nogami (LN) type allows for the mixing of $\boldsymbol{t} = 1$ and $\boldsymbol{t} = 0$ pairing phases, breaking the isospin symmetry. The mixing appears only when the strength $G_{t=0}$ of the average isoscalar pair field exceeds the strength of the isovector field $G_{t=1}$, *i.e.* for $x^{t=0} = G_{t=0}/G_{t=1} \geq x_{\rm crit} \sim 1.1$. The Wigner energy generated through this mechanism contributes to $\lambda^{(2)}_{\tau\,\tau}$ with the sign that is opposite to that in $\lambda^{(2)}_{\tau\,-\tau}$ building up an asymmetry in the auxiliary LN fields: $\lambda^{(2)}_{\tau\tau\prime}\Delta N_\tau \Delta N_{\tau\prime}$.

Since the LN solution does not allow for an isovector *pn*-field, the situation qualitatively resembles the case considered in sect. 4.2. Let us, however, point out that the LN procedure introduces an explicit state dependence of the effective gaps:

$$\Delta_{i\tau\bar{j}\tau\prime} = \Delta_{\tau\tau\prime}\delta_{ij} + 2\lambda^{(2)}_{\tau\tau}\kappa_{i\tau\bar{j}\tau\prime}. \tag{61}$$

Moreover, the LN parameters $\lambda^{(2)}_{\tau\tau\prime}$ are anisotropic in isospace [14]. In turn, a wider class of solutions become possible, including solutions which mix $\boldsymbol{t} = 1$ and $\boldsymbol{t} = 0$ pairing phases and are *collective* in isospace. On the other hand, the absence of the isovector *pn*-field in the LN solutions limits the possibilities to calculate the amplitude of the isovector *pn* pair transfer, see the next section.

6 Proton-neutron pair transfer

The theory of pair transfer/stripping processes like (α, d), $(^3\mathrm{He}, n)$ etc. were developed already in the end of 1950s and at the beginning of 1960s [27–30] based on the plane-wave Born approximation. The general expression for two-nucleon spectroscopic factor (2nSF) carrying nuclear-structure information was derived using the spherical shell model in the jj-coupling limit, see refs. [29,30]. The first analysis of the 2nSF using the pairing interaction model was done by Yoshida [31]. He pointed out the possibility of an enhanced cross-section for the two-particle transfer of the isovector pair due to collective pairing phenomena which may be particularly strong if the coherence of the pairing field extends over few j shells. Based on Yoshida's work, Fröbrich [32,33] has analyzed the influence of *pn* pairing on *pn* pair transfer in $N = Z$ nuclei using both $\boldsymbol{t} = 1$ and $\boldsymbol{t} = 0$ pairing interactions within a single-j shell model space. He pointed out that *pn* pairing can enhance the cross-section by a factor of 3 as compared to conventional shell-model calculations of [34].

In the deformed shell model (paired mean field) the differential cross-section describing the transfer of isoscalar or isovector *pn* pair is proportional to

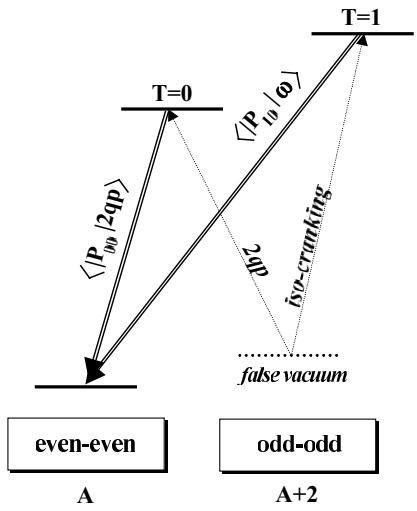

Fig. 2. Schematic figure showing pair transfer and structure of the $T = 0$ and $T = 1$ states in o-o $(A + 2)$ and ground state of e-e (A) $N = Z$ nuclei. The thin arrows indicate the structure of the $T = 0(1)$ states in o-o nuclei in our model, see [16] for detailed discussion. Note that the different structures of the $T = 0$ states imply the quenching of isoscalar pair transfer even for a $\boldsymbol{t} = 0$ paired systems.

$$\frac{\mathrm{d}\sigma}{\mathrm{d}\Omega} \sim |T^{(A,A+2)}_{10(00)}|^2 = |\langle\Psi_A|\boldsymbol{P}_{10(00)}|\Psi_{A+2}(T)\rangle|^2\,, \tag{62}$$

where we have assumed that the transfer goes from the $T = 1(0)$ ground state $|\Psi_{A+2}(T)\rangle$ of the o-o $N = Z = (A + 2)/2$ nucleus to the ground state $|\Psi_A\rangle$ of the even-even nucleus $N = Z = A/2$. Within our model [15–17], $|\Psi_A\rangle$ has the structure of a 0QP state while the structure of $|\Psi_{A+2}(T)\rangle$ depends on the isospin T. For $T = 0$, $|\Psi_{A+2}(T = 0)\rangle$ is a 2QP state while the $|\Psi_{A+2}(T = 1)\rangle$ states maintain the 0QP structure but is cranked in isospace starting from 0QP solution calculated at $\omega_\tau = 0$ which we call *false vacuum*, see [16] and fig. 2. In all cases, the $|\Psi_A\rangle$ and $|\Psi_{A+2}(T)\rangle$ states are described by the fully self-consistent amplitudes $(\boldsymbol{U}^{(A)}\,\boldsymbol{V}^{(A)})$ and $(\boldsymbol{U}^{(A+2)}\,\boldsymbol{V}^{(A+2)})$. Using the generalized Wick's theorem, one can derive the explicit expression for the pair transfer amplitude $T^{(A,A+2)}$ (62):

$$T^{(A,A+2)}_{10(00)} = \frac{1}{\sqrt{2}}\langle\Psi_A|\Psi_{A+2}\rangle \sum_{i>0}\left\{\kappa^{(A,A+2)}_{in,\bar{i}p} \pm \kappa^{(A,A+2)}_{ip,\bar{i}n}\right\}, \tag{63}$$

where

$$\boldsymbol{\kappa}^{(A,A+2)} = (\boldsymbol{V}^{(A+2)})^*(\boldsymbol{U}^T)^{-1}(\boldsymbol{U}^{(A)})^T\,, \tag{64}$$

$$\boldsymbol{U} \equiv (\boldsymbol{U}^{(A+2)})^\dagger\boldsymbol{U}^{(A)} + (\boldsymbol{V}^{(A+2)})^\dagger\boldsymbol{V}^{(A)}\,. \tag{65}$$

The overlap is given by Onishi formula

$$\langle\Psi_A|\Psi_{A+2}\rangle = \sqrt{\mathrm{Det}\boldsymbol{U}}. \tag{66}$$

According to our model, there is a fundamental difference between the structure of the $T = 0$ and $T = 1$ states

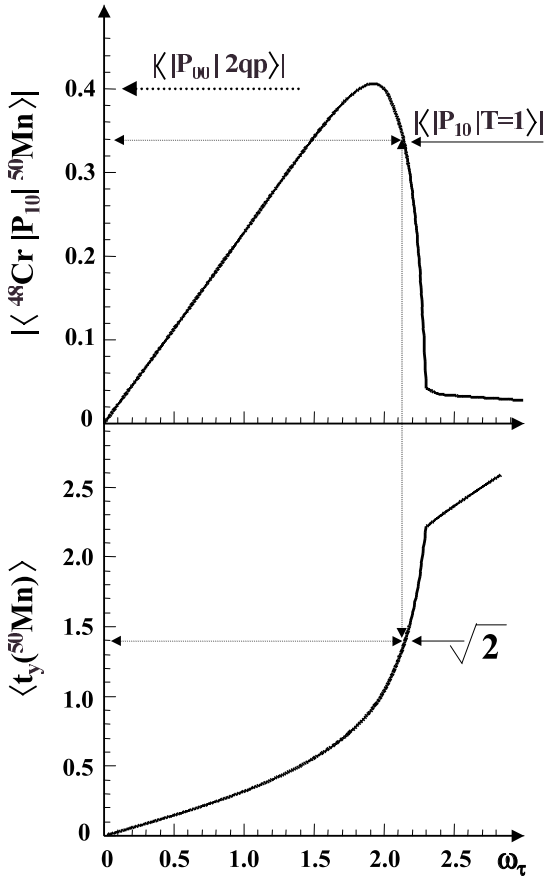

Fig. 3. Isovector *pn* pair transfer $\langle |P_{10}|\omega_\tau\rangle$ (upper part) and iso-alignment (lower part) *versus* ω_τ. The calculations were done in the LN approximation. In this approximation $\boldsymbol{t}=1$ *pn* pairing plays a redundant role [2,14] resulting in the quenching of $\langle |P_{10}|\omega_\tau\rangle$.

in the parent (o-o) nucleus, see fig. 2. The $T=0$ states correspond to 2QP excitations. Therefore, the deuteron will be transferred from a 2QP state to the BCS vacuum in the daughter nucleus. In such a case, the $T_{00}^{(A,A+2)}$ amplitude will essentially probe $\sim (U_A)_i^2$ (i enumerates blocked qp state) and will always be severely quenched [31].

On the other hand, the isovector *pn* pair will be transfered between 0QP states and can, in principle, be enhanced due to the pairing collectivity. The generic situation is illustrated in fig. 3 for the case of ^{48}Cr and ^{50}Mn. In these calculations we assume $x^{t=0}=1.3$ for both the ground state of ^{48}Cr and the *false vacuum* of ^{50}Mn. With increasing ω_τ ^{50}Mn picks up a small fraction of the isovector *pn* pairing and $T_{10}^{(A,A+2)}$ increases reaching maximum around $\langle \hat{t}_y\rangle \sim 1$. (These particular calculations were performed, without loosing generality, for *collective* isorotation around y-axis.) Then in the region of the phase transition it decreases rapidly due to the vanishing overlap, see eq. (63). In the region of $\langle \hat{t}_y\rangle$ $\sim$1 to $\sim\sqrt{2}$ the $|T_{10}^{(A,A+2)}| \sim |T_{00}^{(A,A+2)}| \sim 0.4$, *i.e.* no collective enhancement is calculated for the pair transfer.

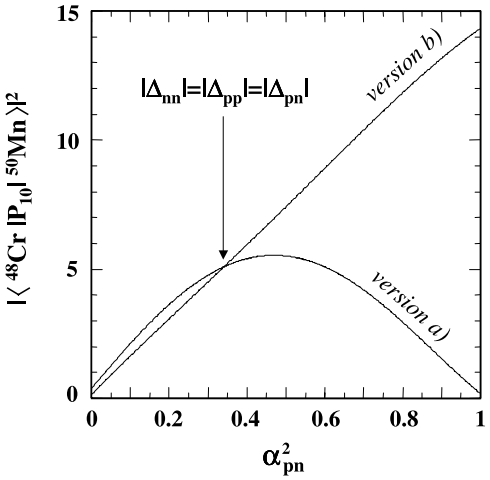

Fig. 4. Pair transfer amplitude $\langle |P_{10}|\rangle$ calculated in the BCS approximation for a model involving $\boldsymbol{t}=1$ correlations only. The results are shown as a function of the contribution of Δ_{pn} to the total gap, see text for details.

The small value of the $T_{10}^{(A,A+2)}$ amplitude is related to the fact that within the LN model the isovector *pn* pairing is essentially not active, see [35] for details. To investigate the importance of isovector *pn* correlations, we have to come back to the $\boldsymbol{t}=1$ pairing model of sect. 3.2. In this case, an analytical expression for the transfer amplitude can be easily derived:

$$\frac{T_{10}^{(A,A+2)}}{\langle \Psi_A|\Psi_{A+2}\rangle} = \frac{e^{i\varphi}}{\sqrt{2}}\sum_{i>0}\left\{\frac{u_{i+}^{(A)^*}v_{i+}^{(A+2)}}{X_i^{(-)}} - \frac{u_{i-}^{(A)^*}v_{i-}^{(A+2)}}{X_i^{(+)}}\right\}, \tag{67}$$

where

$$X_i^{(\pm)} = u_{i\pm}^{(A)^*}u_{i\pm}^{(A+2)} + v_{i\pm}^{(A)^*}v_{i\pm}^{(A+2)}\,. \tag{68}$$

The amplitudes $(\boldsymbol{u},\boldsymbol{v})$ define the Bogolyubov transformation in the canonical basis. They are equal:

$$u_{i\pm} = \sqrt{2}U_{i\pm}^* \qquad \text{and} \qquad v_{i\pm} = \sqrt{2}V_{i\pm}^*\,, \tag{69}$$

where $U_{i\pm}, V_{i\pm}$ are given by eq. (27) (for the daughter nucleus they are obtained at $\omega_\tau = 0$). Let us now assume that $\omega_\tau = 0$. When $\Delta_{pn}=0$, then both $u_+ = u_-$ and $v_+ = v_-$ and we have an exact cancellation of two relatively large terms in the r.h.s of eq. (67). On the other hand, for $\Delta_{pn}\neq 0$, also $u_+ \neq u_-$. Moreover, since $u_\pm \sim \Delta \mp \Delta_{pn}e^{-i\varphi}$ (see eq. (27)) the contributions proportional to Δ_{pn} will add up giving rise to a rapid increase of $|T^{(A,A+2)}|$ as a function of the contribution of the *pn* pair gap to the total gap $\Delta_T^2 \equiv \Delta^2 + |\Delta_{pn}|^2 = \text{const}$. This is shown in fig. 4 in version a). In this version of the calculations α_{pn}^2 $[|\Delta_{pn}|^2 \equiv \alpha_{pn}^2\Delta_T^2]$ was forced to be the same for ^{48}Cr and ^{50}Mn (at $\omega_\tau = 0$). Version b), on the other hand, assumes fixed structure $\Delta = |\Delta_{pn}|$ in ^{48}Cr. In this case, α_{pn}^2 refers to ^{50}Mn. It is clearly seen from the figure that the maximum transfer is expected for similar (but no necessarily equal) content of *pn* pairing in the parent and daughter nucleus. Obviously, other factors like different deformations, etc., may additionally hinder *pn* pair transfer.

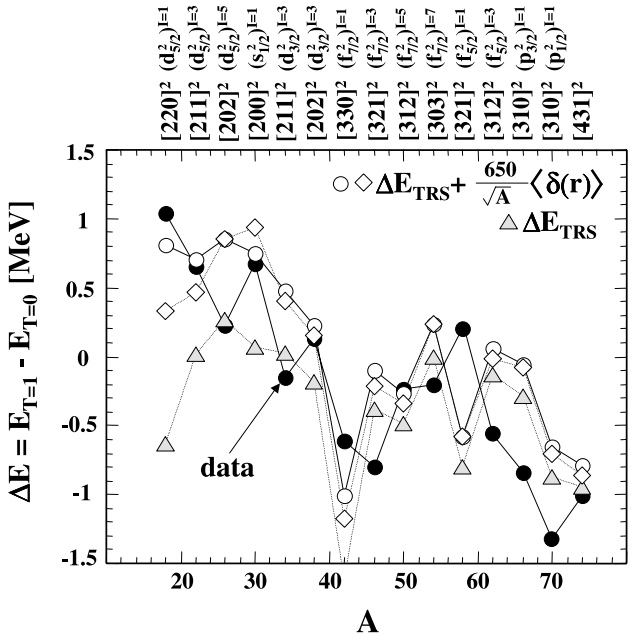

Fig. 5. The difference $\Delta E \equiv E_{T=0} - E_{T=1}$ calculated using the TRS model (triangles). Open circles and diamonds mark the calculations including the correction due to the interaction of the valence particles evaluated assuming Nilsson asymptotic and spherical wave functions, respectively (see text). Solid circles mark the available data which are collected in table 1.

Table 1. The empirical values of excitation energies and spins of the lowest two $T = 0$ and the lowest two $T = 1$ states in o-o $N = Z$ nuclei. Data are taken from: ^{18}F–^{58}Cu ref. [38]; ^{62}Ga ref. [39]; ^{66}As ref. [40]; ^{70}Br ref. [41]; ^{74}Kr ref. [42]. Spin values in brackets are uncertain.

	$E_1^{T=0}$	$E_2^{T=0}$	$E_1^{T=1}$	$E_2^{T=1}$
$^{6}_{3}$Li$_3$	0 (1^+)	2.185 (3^+)	3.562 (0^+)	5.370 (2^+)
$^{10}_{5}$B$_5$	0 (3^+)	0.718 (1^+)	1.742 (0^+)	5.163 (2^+)
$^{14}_{7}$N$_7$	0 (1^+)	4.915 (0^-)	2.313 (0^+)	8.062 (1^-)
$^{18}_{9}$F$_9$	0 (1^+)	0.937 (3^+)	1.041 (0^+)	3.061 (2^+)
$^{22}_{11}$Na$_{11}$	0 (3^+)	0.583 (1^+)	0.657 (0^+)	1.952 (2^+)
$^{26}_{13}$Al$_{13}$	0 (5^+)	0.417 (3^+)	0.228 (0^+)	2.070 (2^+)
$^{30}_{15}$P$_{15}$	0 (1^+)	0.709 (1^+)	0.677 (0^+)	2.938 (2^+)
$^{34}_{17}$Cl$_{17}$	0.146 (3^+)	0.461 (1^+)	0 (0^+)	2.158 (2^+)
$^{38}_{19}$K$_{19}$	0 (3^+)	0.459 (1^+)	0.130 (0^+)	2.403 (2^+)
$^{42}_{21}$Sc$_{21}$	0.611 (1^+)	0.617 (7^+)	0 (0^+)	1.586 (2^+)
$^{46}_{23}$V$_{23}$	0.801 (3^+)	0.915 (1^+)	0 (0^+)	0.993 (2^+)
$^{50}_{25}$Mn$_{25}$	0.230 (5^+)	0.651 (1^+)	0 (0^+)	0.800 (2^+)
$^{54}_{27}$Co$_{27}$	0.199 (7^+)	0.937 (1^+)	0 (0^+)	1.447 (2^+)
$^{58}_{29}$Cu$_{29}$	0 (1^+)	0.445 (1^+)	0.203 (0^+)	1.652 (2^+)
$^{62}_{31}$Ga$_{31}$	0.571 (1^+)	0.818 (3^+)	0 (0^+)	
$^{66}_{33}$As$_{33}$	0.837 [1^+]	1.231 (3^+)	0 (0^+)	0.963 [2^+]
$^{70}_{35}$Br$_{35}$	1.337 (3^+)	1.653 (5^+)	0 (0^+)	0.934 (2^+)
$^{74}_{37}$Rb$_{37}$	1.006 [3^+]	1.224 [4^+]	0 [0^+]	0.478 [2^+]

7 Total-Routhian-Surface calculations including isoscalar pairing

We have performed systematic calculations of the energy differences $\Delta E \equiv E_{T=0} - E_{T=1}$ between the lowest $T = 0$ and $T = 1$ states in o-o $N = Z$ nuclei using the Total-Routhian-Surface (TRS) method. We used the deformed Woods-Saxon potential and included both isovector and isoscalar pairing treated in the LN approximation. The deformation space covered quadrupole β_2, γ and hexadecapole β_4 shapes. The liquid-drop formula of [36] was used to calculate the macroscopic part of the total energy. Apart from including $\boldsymbol{t} = 0$ pairing, the details of the method follow our standard implementation and we refer the reader to ref. [37] for further details.

The calculations have been done for all o-o $N = Z$ nuclei from ^{18}F to ^{74}Rb. To account for the $T = 0$ states, the 2QP surfaces $\alpha_1^\dagger\alpha_2^\dagger|0\rangle$ have been created, where $\alpha_{1(2)}^\dagger$ denote the lowest qp states of the same signature. We use the notion of signature rather than time reversal since the calculations have been done at a small fixed spatial rotational frequency. By blocking $\alpha_1^\dagger\alpha_2^\dagger|0\rangle$ we assure that all pairing fields are truly blocked. Indeed, blocking the lowest qp states of opposite signatures $\alpha_1^\dagger\alpha_{\bar{1}}^\dagger|0\rangle$ results in the blocking of isovector *pp* and *nn* pairing but not isoscalar *pn* pairing. It is assumed that the valence blocked quasi-particles (proton-neutron) may interact. This interaction is added as a perturbation assuming a simple (isoscalar) delta-force $g(A)_{\rm eff}\delta(\boldsymbol{r}_1 - \boldsymbol{r}_2)$ as a residual interaction. For further simplification we assume either spherical $|(nljm)^2; I\rangle$ or Nilsson asymptotic $|(Nn_z\Lambda K)^2\rangle$ limits for the two-body wave function with I or $2K$ equal to empirical spin $I_{\rm exp}$. An effective strength of the residual force $g(A)_{\rm eff} = g_{\rm eff}/\sqrt{A}$ was assumed. This gives rise to a $\sim 1/A$-dependence for the matrix element in accordance to the standard mass dependence of the valence *pn* interaction energy in liquid-drop models [43].

The $T = 1$ states were calculated in a slightly simplified manner. Self-consistent TRS calculations have been done for the 0QP state (*false vacuum*) at $\omega_\tau = 0$. Then, the iso-cranking calculations were performed at the deformation corresponding to a minimum of the TRS calculations.

The TRS calculations have been performed for a slightly reduced strength of the pairing force as compared to the estimate of [15]. The TRS and δ-force corrected TRS results are presented in fig. 5. The strength of the δ-force $g_{\rm eff} \sim 650\,$MeV was estimated from a least-square fit to the data. The size of the matrix element is more or less consistent with an average liquid-drop estimate of $\sim 20/A\,$MeV of the *pn* effect for valence particles in o-o nuclei although one would expect an enhancement in $N = Z$ nuclei purely due to geometrical reason (congruence effect). However, the overall quality of the fit does not change very much even if we double $g_{\rm eff}$ and therefore is not very conclusive.

The new elements in these calculations with respect to the one presented in ref. [16] can be summarized as follows: i) the equilibrium deformation is calculated from the TRS

minimum; ii) two quasi-particles of the same type (*i.e.* not in time-reversed states) have been blocked and the residual *pn* interaction between the valence pair has been added to the energy difference to reduce the coherence of the $\boldsymbol{t} = 0$ pair field. These new calculations describe well the global decrease of $\Delta E(A)$ including the sign inversion in the $f_{7/2}$ shell, see fig 5. However, the details are far from being satisfactorily reproduced. More extended studies of the wave function of the valence nucleons is not expected to improve the situation, since the TRS ground states are essentially spherical for light nuclei. Deformation sets in only for heavy nuclei where spherical and asymptotic matrix elements of the δ-force are anyhow very similar. This seems to indicate that the $\boldsymbol{t} = 0$ pairing needs further reduction.

8 Influence of isovector particle-hole fields on the moment of inertia in isospace

Phenomenological potentials (like the Woods-Saxon potential used here) depend only on the third component of the isospin $I = (N - Z)/A$. It means that essentially no modification of the mean field is obtained as a function of excitation energy in a given nucleus. On the contrary, such modifications are automatically included in self-consistent approaches through the changes of the isovector densities.

The presence of a repulsive isovector mean field provides an alternative (or additional) mechanism to lower the MoI in isospace. Let us illustrate it by using the simple iso-cranked single-particle model discussed in detail in refs. [15–17] and including an additionally repulsive two-body interaction $\frac{1}{2}\kappa\hat{\boldsymbol{t}} \cdot \hat{\boldsymbol{t}}$ analyzed by Neergård [26]:

$$\hat{H}^{\omega} = \hat{h}_{\rm sp} - \vec{\boldsymbol{\omega}}\vec{\hat{\boldsymbol{t}}} + \frac{1}{2}\kappa\hat{\boldsymbol{t}} \cdot \hat{\boldsymbol{t}}. \tag{70}$$

Linearization of the Hamiltonian (70) and simultaneous assumption of one-dimensional rotation (say, around the x-axis, then $\langle\hat{t}_y\rangle = \langle\hat{t}_z\rangle = 0$) leads effectively to a one-dimensional mean-field cranking Hamiltonian:

$$\hat{H}^{\omega}_{\rm MF} = h_{\rm sp} - (\omega - \kappa\langle\hat{t}_x\rangle)\hat{t}_x \tag{71}$$

with an effective isospin-dependent cranking frequency. The role of the isovector field is depicted schematically in fig. 6, where for simplicity the equidistant sp spectrum $e_i = i\delta e$ for $h_{\rm sp} = \sum_{\rm occ} e_i$ is assumed. It is clearly seen from the figure that the isovector field simply shifts crossing frequencies from $\delta e, 3\delta e, 5\delta e, \ldots$ to $\delta e+\kappa, 3(\delta e+\kappa), 5(\delta e+\kappa), \ldots$. These shifts are marked by dashed lines in fig. 6, since they are in fact instantaneous due to noncollective iso-cranking. The energy dependence $E(T)$ as a function of isospin $[T = T_x \equiv \langle\hat{t}_x\rangle]$ reads:

$$E(T) = \frac{1}{2}(\delta e + 2\kappa)T^2\,, \tag{72}$$

i.e. is analogical to the one derived in [15] but with a reduced MoI-i. Adding standard $\boldsymbol{t} = 1, t_z = \pm 1$ pairing with $\Delta_n = \Delta_p$ *deforms* the system (see sect. 3) and smooths

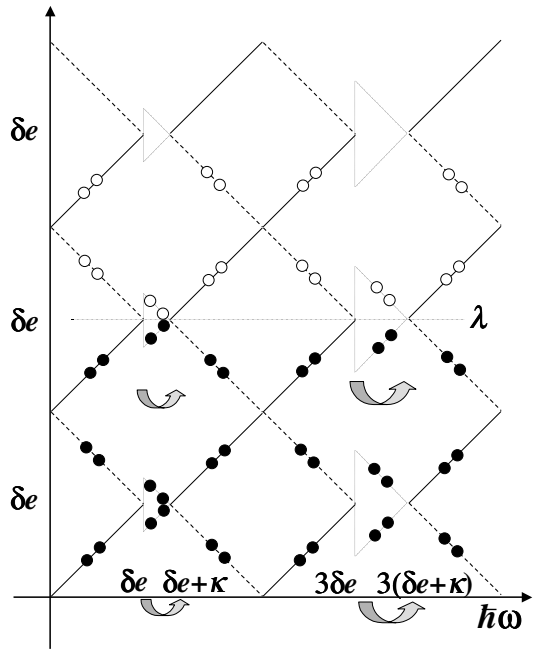

Fig. 6. Single-particle Routhians for the model described by the Hamiltonian (71). Filled circles mark occupied states. Arrows indicate shifts in crossing frequencies due to the isospin dependence introduced via the $\frac{1}{2}\kappa\hat{\boldsymbol{t}} \cdot \hat{\boldsymbol{t}}$ interaction.

out the single-particle, step-like alignment process (*collective iso-rotation*) but does not essentially change the MoI-i as demonstrated in [15–17] (see also sect. 3.2). The *collectivity* introduced by the $\boldsymbol{t} = 1, t_z = \pm 1$ pairing correlations allows for incorporating isospin fluctuations in a static way through the standard cranking condition

$$E = \frac{1}{2}(\delta e + 2\kappa)T^2 \longrightarrow \frac{1}{2}(\delta e + 2\kappa)T(T+1). \tag{73}$$

Evidently, the linear term is increased in the presence of the isovector potential. This regime of the model with fixed A, and $T_z = 0$ can be called the *vertical*-excitation regime. Changing the iso-cranking generator from $\hat{t}_x$ to $\hat{t}_z$ and constraining the total particle number A, only brings our model to the regime of *horizontal* excitations describing ground states of neighboring nuclei of the same A. The mathematics used to solve both models is identical. Note, however, that the physics interpretation changes. For example, the physical restrictions for allowed sp (or qp) excitations which were related to iso-signature conservation and time-reversal symmetries [15–17] now can be interpreted in terms of neutron and proton number parities [8]. The cranking frequency measures the difference between neutron and proton Fermi energies.

In the derivation of eq. (72), the isovector Hartree potential $V_T = \kappa\langle\hat{\boldsymbol{t}}\rangle\hat{\boldsymbol{t}}$ was used rather than the two-body interaction. This seems to be consistent with the standard potential-like treatment of the isovector terms in phenomenological nuclear potentials. In such a case, use of the cranking condition (73) is justified. Since for large isospins *pn* pairing is irrelevant, the inertia parameter (the symmetry energy strength $a_{\rm sym}$) is fully determined by the

Table 2. Results of the least-square fit for the Wigner energy strength $E_{\rm wig} = a_{\rm wig}|N-Z|/A^{\alpha}$ and for the symmetry energy strength $E_{\rm sym} = a_{\rm sym}(N-Z)^2/A^{\alpha}$. The minimum of the mean standard deviation is reached at $\alpha \sim 0.95$ for both Wigner energy and symmetry energy fits. Results of one-dimensional fits at fixed $\alpha = 1/2;\ 2/3;\ 1$ are given for comparison.

α	$a_{\rm wig}$	σ_{n-1}	$2a_{\rm sym}$	σ_{n-1}	$x = a_{\rm wig}/2a_{\rm sym}$
0.95	39	0.196	31	0.106	1.26
1/2	8	0.239	6	0.153	1.33
2/3	14	0.213	11	0.125	1.27
1	47	0.196	38	0.107	1.24

mean-level density and κ. The data does not give any signature of enhancement of $a_{\rm sym}$ in $N = Z$ nuclei. Still isoscalar *pn* pairing effects may be related to the enhancement of the *linear* term to $\frac{1}{2}a_{\rm sym}T(T+x)$ with $x > 1$.

The symmetry energy strength, and indirectly the value of κ, can be conveniently fitted using the so-called double difference $V_{pn} \approx \frac{\partial^2 B}{\partial N \partial Z}$ formula [44]. The results of a local fit to $N \sim Z$ nuclei involving $Z \geq 10$, $1 \leq T_Z \leq 3$ nuclei (except o-o $T_Z = 1$ nuclei) are shown in table 2. This fit assumes $E_{\rm sym} \propto (N-Z)^2$ since the linear term vanishes because of the second derivative. However, the strength of the linear term (or the Wigner energy $E_{\rm wig} \propto |N-Z|$) can be fitted separately using the prescription of ref. [35] which gives information about the local enhancement factor x in the $E_{\rm sym} \sim T(T+x)$ formula.

The obtained strength of the symmetry energy lies in between large scale fits of $E_{\rm sym} \sim T^2$ type [45] and with those assuming $E_{\rm sym} \sim T(T+1)$. The latest gives

$$E_{\rm sym} = \left(134.4 - \frac{203.6}{A^{1/3}}\right)\frac{T(T+1)}{A}\,{\rm MeV} \approx \frac{1}{2}160\frac{T(T+1)}{A}\,{\rm MeV} \qquad (74)$$

for $A \sim 50$ [46]. The data show clear enhancement of the linear term with $x \sim 1.25$ (last column) which is consistent with the early findings of Jänecke [47]. Indeed, it clearly leaves room for isoscalar pairing since isospin fluctuations in the static theory limit gives $x = 1$ by definition.

We have recently [48] demonstrated that the schematic interaction (70) captures many features of realistic effective isovector interactions. In particular, in the Hartree-Fock limit, it gives rise to a *linear term* in the symmetry energy:

$$\frac{1}{2}\kappa\langle\Delta\hat{\boldsymbol{t}}^2\rangle \xrightarrow{\rm HF} \frac{1}{2}\kappa T. \qquad (75)$$

This term is only due to the isovector part of the mean HF potential and therefore represents only a fraction of the *linear term*. The mean-level density related contribution

$$\frac{1}{2}\varepsilon\langle\Delta\hat{\boldsymbol{t}}^2\rangle \qquad (76)$$

seems to go beyond the mean-field approximation and its microscopic evaluation requires RPA calculations [26].

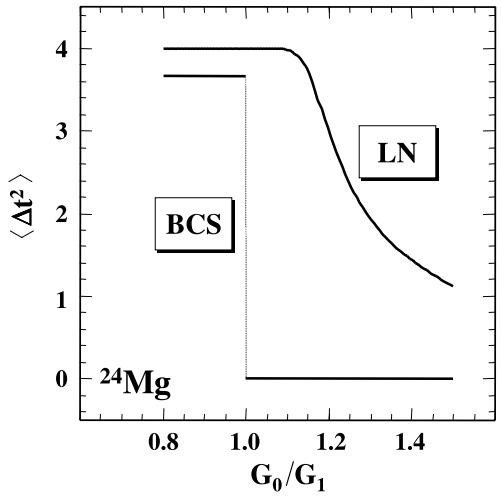

Fig. 7. Dispersion in isospin $\langle\Delta\hat{\boldsymbol{t}}^2\rangle$ calculated for the LN and BCS models as a function of the ratio of the strengths of isoscalar to isovector pairing forces. Note that $\boldsymbol{t} = 0$ pairing strongly quenches $\langle\Delta\hat{\boldsymbol{t}}^2\rangle$. In particular, in the limit of pure isoscalar pairing (BCS) $\langle\Delta\hat{\boldsymbol{t}}^2\rangle = 0$.

Standard *pp*/*nn* pairing leads to a strong quenching of the linear term (75), as compared to its sp estimate [48]. Since κ is fixed for a schematic force, the suppression of this term is entirely due to the enhancement of the $T/\langle\Delta\hat{\boldsymbol{t}}^2\rangle$ ratio. This mechanism may also quench the linear term (76). Therefore, from a microscopic point of view, one would expect $x < 1$, *i.e.* below the static estimate. For example, Neergård [26] gives $x \sim 0.8$ for $T = 2$, $A = 48$ nuclei. Let us point out, however, that his estimate is based on a mean-level splitting deduced from the Fermi-gas model which is unrealistically large as shown in [48].

Moreover, Neergård's model is oversimplified, since it neglects $\boldsymbol{t} = 0$ pairing correlations. These correlations, even by entering at the dynamical RPA level, are expected to reduce isospin fluctuations as they in fact do in the static BCS or LN theory, see fig. 7. In conclusion, as expected, the presence of an isovector particle-hole field will reduce isoscalar pairing effects but it does not rule out their existence in $N \sim Z$ nuclei.

9 Summary and conclusions

We present analytical solutions for a model including schematic isovector and isoscalar pairing and discuss in detail the response of the $\boldsymbol{t} = 1$ and $\boldsymbol{t} = 0$ pair fields to rotations in isospace in $N = Z$ nuclei. We are particularly interested in the relations of the gauge angles of the $\boldsymbol{t} = 1$ pair gaps and the position of the cranking axis in isospace. These relations decide upon the character of rotation in isospace. In particular, it is shown that within the model including standard *nn* and *pp* pair correlations and under the assumption of eq. (12), no tilted solutions are possible. Iso-rotation is either of collective type $\vec{\boldsymbol{\Delta}} \perp \vec{\boldsymbol{\omega}}$ or noncollective type $\vec{\boldsymbol{\Delta}} \parallel \vec{\boldsymbol{\omega}}$. Since iso-rotation in $N = Z$ nuclei is planar, the *pn* $\boldsymbol{t} = 1$ pair field always induces collectivity

(triaxial deformation). Again, it is shown that the most general solutions are obtained for pure collective cases when the $\boldsymbol{t} = 1$ pair field $[\boldsymbol{\Delta}_{\perp}, \boldsymbol{\Delta}_{pn}]$ is perpendicular to the iso-cranking axis, *i.e.* when $\vec{\boldsymbol{\Delta}}_{\perp} \perp \vec{\boldsymbol{\omega}}$. Other solutions may be possible only for particular values of the gaps.

We also demonstrate that models using simple schematic pairing interactions, mixing of $\boldsymbol{t} = 1$ and $\boldsymbol{t} = 0$ correlations are essentially forbidden or more precisely restricted to a very special combination of the pair gaps. This is due to the different phase structure of the eigenvectors among time-reversed states, compare eq. (10) and eq. (43), or alternatively, due to the different transformation properties of $\boldsymbol{t} = 1$ and $\boldsymbol{t} = 0$ gaps under time reversal.

Numerical calculations show that this mixing is allowed within the HFB approximation but only for more complicated pairing interactions [5,11]. It is also possible for schematic interactions, within the LN approximation [2]. In the latter approximation, however, the *pn* $\boldsymbol{t} = 1$ pair gap vanishes, which makes it unsuitable to calculate the $T = 1$ pair transfer between the $T = 1$ o-o ground state and $T = 0$ e-e vacuum. Let us point out very clearly that, since $T = 1$ o-o ground state and $T = 0$ e-e vacuum are, according to our interpretation, both 0QP states, the $\boldsymbol{t} = 1$ pair transfer can in principle become enhanced through $\boldsymbol{t} = 1$ *pn* correlations as demonstrated within the BCS approximation in sect. 6. On the other hand, the fundamental difference in structure between the $T = 0$ vacua in e-e and o-o nuclei results in a quenching of the $T = 0$ pair transfer even in the presence of strong $\boldsymbol{t} = 0$ pairing.

The energy difference of $\Delta E \equiv E_{T=0} - E_{T=1}$ can be reproduced in a schematic manner by our extended TRS calculations, including a residual *pn* interaction of δ-type. Some discrepancies remain, most likely related to the fact that the $\boldsymbol{t} = 0$ pairing is too strong in our calculations due to the lack of particle-hole isovector interaction. Inclusion of such an interaction will result in a weakening of the isoscalar pairing. However, the enhancement in binding energy in $N = Z$ as compared to $N - Z = 2$ nuclei seems to leave quite some room for $\boldsymbol{t} = 0$ pair correlations as discussed in sect. 8. Further work along this line is in progress.

This work was supported by the Göran Gustafsson Foundation, the Swedish Institute, the Polish Committee for Scientific Research (KBN) under Contract No. 5 P03B 014 21, and by the U.S. Department of Energy under Contract Nos. DE-FG02-96ER40963 (University of Tennessee), and DE-AC05-00OR22725 (UT-Battelle).

References

1. J. Engel, K. Langanke, P. Vogel, Phys. Lett. B **389**, 211 (1996).
2. W. Satuła, R. Wyss, Phys. Lett. B **393**, 1 (1997).
3. J. Engel, S. Pittel, M. Stoitsov, P. Vogel, J. Dukelsky, Phys. Rev. C **55**, 1781 (1997).
4. D.J. Dean, S.E. Koonin, K. Langanke, P.B. Radha, Phys. Lett. B **399**, 1 (1997).
5. J. Terasaki, R. Wyss P.-H. Heenen, Phys. Lett. B **437**, 1 (1998).
6. J. Dobes, S. Pittel, Phys. Rev. C **57**, 688 (1998).
7. S. Frauendorf, J. Sheikh, Phys. Rev. C **59**, 1400 (1999).
8. S. Frauendorf, J. Sheikh, Nucl. Phys. A **645**, 509 (1999).
9. K. Kaneko, M. Hasegawa, Phys. Rev. C **60**, 024301 (1999).
10. J. Sheikh, R. Wyss, Phys. Rev. C **62**, 51302(R) (2000).
11. A.L. Goodman, Phys. Rev. C **60**, 014311 (1999).
12. A. Petrovici, K.W. Schmidt, A. Faessler, Nucl. Phys. A **647**, 197 (1999).
13. G. Röpke, A. Schnell, P. Schuck, U. Lombardo, Phys. Rev. C **61**, 024306 (2000).
14. W. Satuła, R. Wyss, Nucl. Phys. A **676**, 120 (2000).
15. W. Satuła, R. Wyss, Phys. Rev. Lett. **86**, 4488 (2001).
16. W. Satuła, R. Wyss, Phys. Rev. Lett. **87**, 052504 (2001).
17. W. Satuła, R. Wyss, Acta Phys. Pol. B **32**, 2441 (2001).
18. H.T. Chen, H. Müther, A. Faessler, Nucl. Phys. A **297**, 445 (1978).
19. R.A. Broglia, A. Winther, *Frontiers in Physics: A Lecture Note and Reprint Series 52* (Benjamin/Cummings, Reading, Mass., 1981).
20. D. Bes, R.A. Broglia, O. Hansen, O. Nathan, Phys. Rep. **34**, 53 (1977).
21. D. Bes, O. Civitarese, E.E. Maqueda, N.N. Scoccla, Phys. Rev. C **61**, 024315 (2000).
22. A.O. Macchiavelli *et al.*, Phys. Rev. C **61**, 041303R (2000).
23. P. Ring, P. Schuck, *The Nuclear Many Body Problem* (Springer-Verlag, New York, 1980).
24. J.N. Ginocchio, J. Weneser, Phys. Rev. **170**, 859 (1968).
25. A.L. Goodman, Nucl. Phys. A **186**, 475 (1972).
26. K. Neergård, Phys. Lett. B **537**, 287 (2002).
27. M. El Nadi, Proc. Phys. Soc. **70**, 62 (1957).
28. M. El Nadi, M. El Khishin, Proc. Phys. Soc. **73**, 705 (1959).
29. H.C. Newns, Proc. Phys. Soc. **76**, 489 (1960).
30. N.K. Glendenning, Nucl. Phys. **29**, 109 (1962).
31. S. Yoshida, Nucl. Phys. **33**, 685 (1962).
32. P. Fröbrich, Z. Phys. **236**, 153 (1970).
33. P. Fröbrich, Phys. Lett. B **37**, 338 (1971).
34. D. Fleming, J. Cerny, C. Maples, N.K. Glendenning, Phys. Rev. **166**, 1012 (1968).
35. W. Satuła, D. Dean, J. Gary, S. Mizutori, W. Nazarewicz, Phys. Lett. B **407**, 103 (1997).
36. W.D. Myers, W. Swiatecki, Nucl. Phys. **81**, 1 (1966).
37. W. Satuła, R. Wyss, P. Magierski, Nucl. Phys. A **578**, 45 (1994).
38. R. Firestone *et al.*, *Table of Isotopes*, 8th edition (Wiley, New York, 1996.).
39. S.M. Vincent *et al.*, Phys. Lett. B **437**, 264 (1998).
40. R. Grzywacz *et al.*, Nucl. Phys. A **682**, 41 (2001)c.
41. D.G. Jenkins *et al.*, Phys. Rev. C **65**, 064307 (2002).
42. D. Rudolph *et. al.*, Phys. Rev. Lett. **76**, 376 (1996).
43. H.J. Krappe, J.R. Nix, A.J. Sierk, Phys. Rev. C **20**, 992 (1979).
44. J.-Y. Zhang, R.F. Casten, D.S. Brenner, Phys. Lett. B **227**, 1 (1989).
45. P. Möller, J.R. Nix, W.D. Myers, W.J. Swiatecki, At. Data Nucl. Data Tables **59**, 185 (1995).
46. M. Duflo, A.P. Zucker, Phys. Rev. C **52**, R23 (1995).
47. J. Jänecke, Nucl. Phys. **73**, 97 (1965).
48. W. Satuła, R. Wyss, Phys. Lett. B **572**, 152 (2003), LANL preprint nucl-th/0211044.